Acta Cryst. (1978). B**34**, 2487–2494

Electron-Density Distribution in Crystals of Diformohydrazide

BY KIYOAKI TANAKA

The Research Laboratory of Engineering Materials, Tokyo Institute of Technology, O-okayama, Meguro-ku, Tokyo 152, *Japan*

(*Received* 14 *May* 1977; *accepted* 9 *January* 1978)

The electron-density distribution in crystals of OHC–HN–NH–CHO was calculated on the basis of the intensity data collected by diffractometry at 23 °C. The crystals are monoclinic, $P2_1/a$, with the cell dimensions $a = 8{\cdot}987$ (1), $b = 6{\cdot}2617$ (7), $c = 3{\cdot}5846$ (7) Å, $\beta = 113{\cdot}05$ (2)°, and $Z = 2$. The crystal and molecular structure agrees well with those reported previously. The numbers of electrons around each atom or atomic group estimated by direct integration of the observed electron density in an appropriate volume are: NH = 7·85, CH = 6·76, N = 6·50, C = 5·45 and O = 8·41. This result is compared with that of a CNDO/2 calculation. The errors in electron-density and residual-electron-density maps are discussed to assess the intermolecular electron density on the N–H···O hydrogen bond, and the residual features of asphericity due to bonding and lone-pair electrons.

Introduction

Diformohydrazide comprises important functional groups in biochemistry; moreover, the molecules in the crystalline state are held together by N–H···O hydrogen bonds that play an important role in protein chemistry. The crystal structure of diformohydrazide had been studied carefully on the basis of two-dimensional data collected by photographic methods by Tomiie, Koo & Nitta (1958). They also estimated the number of electrons around O, NH and CH, and Tomiie (1958) compared the results with those of molecular-orbital calculations. Recently, Ottersen (1974) redetermined the structure at 19 and −165 °C. He carried out L shell and extended L shell (ELS) refinement based on the contracted Gaussian-type orbitals (Ottersen, 1974; Ottersen & Jensen, 1975). The present study was initiated quite independently from that of Ottersen, which came to our attention after our measurements had been taken. The results based on the intensity data measured by diffractometry at 23 °C exceeded Ottersen's in accuracy, the standard deviations in bond lengths and angles being about $\frac{1}{3}$ those of the former. Thus it was decided to estimate the number of electrons around each atom or atomic group by direct integration of the observed electron density in an appropriate volume, in order to compare the results with those of Ottersen and Tomiie *et al.*, and also to see the bonding effects on the final difference maps.

Experimental

Diformohydrazide was synthesized according to the method described by Ainsworth & Jones (1955). The crystal data are: $C_2H_4N_2O_2$, FW 88·066, monoclinic, $a = 8{\cdot}987$ (1), $b = 6{\cdot}2617$ (7), $c = 3{\cdot}5846$ (7) Å, $\beta = 113{\cdot}05$ (2)°, $U = 185{\cdot}62$ Å^3 (at 23 °C), $D_x = 1{\cdot}576$ g cm^{-3}, $Z = 2$, μ(Mo $K\alpha$, $\lambda = 0{\cdot}71069$ Å) = 1·71 cm^{-1}, space group $P2_1/a$. The cell dimensions agree with those reported by Ottersen (1974) and Tomiie *et al.* (1958), within the experimental errors.

Prior to the intensity data collection, the homogeneity of the incident X-ray beam was checked. A Pb plate 1 mm thick with a pinhole of diameter about 0·1 mm was attached to the two-dimensional micrometer and was allowed horizontal and vertical translations every 0·05 mm and the incident-beam intensity passing through the pinhole was counted. The counter with the vertical receiving slit (0·5 mm wide) scanned at the rate 4° min^{-1} around $2\theta = 0°$ for 30 s. The homogeneous areas in the beam with intensity greater than 90% of the maximum intensity at take-off angles from 3 to 6° were almost circular, with diameters ranging from 0·45 to 0·49 mm. Though the most homogeneous beam was obtained at the take-off angle of 3°, the beam at 5° was

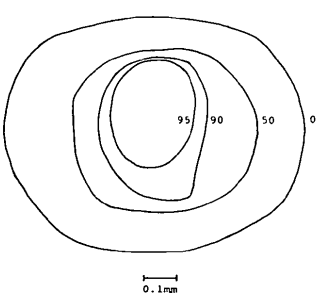

Fig. 1. The intensity distribution of the monochromated incident X-ray beam at a take-off angle of 5°. Numbers show the ratio of the intensity at each contour to the maximum intensity of the beam.

Table 1. *Experimental conditions*

Diameter of specimen	0·33 mm
X-ray tube	Philips PW 205362
Radiation	Mo $K\alpha$, 40 kV, 20 mA
Monochromator	Graphite (002)
Collimator	0·5 mmø × 150 mm
Detector aperture	7·0 mmø
$2\theta_{max}$	135·3°
Background counting	Varied with peak intensity (see text)
Scan technique	ω–2θ scan
Scan width (degrees in 2θ)	$1{\cdot}2 + 0{\cdot}5 \tan\theta \sim 1{\cdot}35 + 0{\cdot}6 \tan\theta$
Maximum number of repetitions	10
Criterion to terminate repetition	$\sigma F/\lvert F\rvert \leq 0{\cdot}01$
Number of observed reflexions	5623

selected for the present data collection because its intensity was 1·5 times more intense than that at 3°. The homogeneity of the X-ray beam monochromated by a graphite (002) plane at a take-off angle of 5° is shown in Fig. 1. It was expected that with the crystal specimen of diameter less than 0·3 mm, the total illumination of X-rays would be practically unchanged during the intensity data collection.

A Rigaku automated four-circle X-ray diffractometer was used for intensity measurements. The crystal was shaped into a sphere by gently rubbing on a piece of wet filter paper. Experimental conditions are summarized in Table 1. The ratio background to peak counting times was varied for each reflexion in proportion to the square root of the ratio between their mean counting rates (Shoemaker, 1968). To avoid counting loss, a Ni-foil attenuator of appropriate thickness was automatically inserted when the diffracted-beam intensity exceeded 5000 counts s^{-1} in a pulse-detecting circuit. The attenuation factors of the five pieces of foil used in the experiment were calculated by employing a least-squares fit to the function obtained by Fukamachi (1969). Their errors derived from the variances of the least-squares fit were less than 0·2% of their attenuation factors. Intensities of all four symmetry-related reflexions (hkl,$h\bar{k}l$,$\bar{h}k\bar{l}$,$\bar{h}\bar{k}\bar{l}$) were collected in succession to avoid random errors during the measurement. Three reference reflexions were measured about every two hours throughout the experiment.

Correction of the intensity data

Observed structure factors F_o were corrected for Lorentz and polarization factors, and also for absorption (the crystal was assumed to be a sphere of radius 0·165 mm). The correction for simultaneous-reflexion effects was made with the method described by Tanaka & Saito (1975); the maximum value of the correction was as large as 16% of a structure factor, and the number of reflexions perturbed more than 1% of their structure factors was 62, among 2266 Friedel pairs. Extinction effects were corrected by the methods of Zachariasen (1967) and Coppens & Hamilton (1970) using the program *LINUS*; only five strong reflexions were perturbed more than 1% of their structure factors. The specimen used in the experiment shows only a minor indication of secondary extinction.

Refinement and description of the structure

The values of F_o for each Friedel pair were averaged to yield 2332 non-zero reflexions (hkl,$h\bar{k}l$); Friedel pairs are perturbed equally by absorption, secondary-extinction and simultaneous-reflexion effects because of the spherical shape of the crystal. In the averaging process, if the intensity of one of the pair was zero, that pair was omitted in the subsequent calculation. The atomic scattering factors of C, N and O atoms calculated by Fukamachi (1971), on the assumption of spherical electron distribution around atoms using the wave functions obtained by Clementi (1965), and that of H by Stewart, Davidson & Simpson (1965) were used. The atomic parameters reported by Tomiie *et al.* (1958) were used as a starting set. After the full-matrix least-squares refinement, which includes the correction for type II anisotropic extinction (that is, extinction dominated by mosaic block size), the usual agreement indices $R_1 = w \sum (\lvert F_o\rvert - \lvert F_c\rvert)/\sum \lvert F_o\rvert$ and $R_2 = [\sum w(\lvert F_o\rvert - \lvert F_c\rvert)^2/\sum wF_o^2]^{1/2}$ reduced to 0·033 and 0·032, respectively, for 2332 Friedel pairs. Finally, these reflexions were further averaged to yield 1244 independent reflexions and for these data sets the R_1 and R_2 values became 0·033 and 0·030. The atomic parameters and type II anisotropic extinction parameters are listed in Tables 2 and 3 respectively.*

The diformohydrazide molecule is planar and centrosymmetric. The equation of the molecular plane is $-5{\cdot}794x + 2{\cdot}077y + 3{\cdot}174z = 0$, where x, y and z are fractions of the lattice constants a, b and c respectively. The deviations of atoms from this plane are: N −0·0028, C 0·0021, O −0·0010, H(1) 0·0253, and H(2) 0·0171 Å.

Bond lengths and angles are shown in Fig. 2. The N—N bond length is evidently shorter than that in other hydrazine derivatives, indicating double-bond character, as already cited (Tomiie *et al.*, 1958; Ottersen,

* A list of structure factors has been deposited with the British Library Lending Division as Supplementary Publication No. SUP 33403 (10 pp.). Copies may be obtained through The Executive Secretary, International Union of Crystallography, 5 Abbey Square, Chester CH1 2HU, England.

Table 2. *Final fractional atomic coordinates and thermal parameters* (Å²)

Values are × 10^5, except those for H, which are × 10^4 for positional and × 10^3 for isotropic thermal parameters. The form of the anisotropic temperature factor is

$$\exp[-2\pi^2(h^2a^{*2}U_{11} + k^2b^{*2}U_{22} + l^2c^{*2}U_{33} + hka^*b^*U_{12} + hla^*c^*U_{13} + klb^*c^*U_{23})].$$

	x	y	z	U_{11}	U_{22}	U_{33}	U_{12}	U_{13}	U_{23}
N	324 (4)	10369 (6)	−6251 (12)	1837 (12)	2259 (14)	2712 (16)	−96 (21)	−187 (22)	413 (24)
C	13796 (5)	21638 (7)	11064 (15)	2239 (16)	2271 (16)	2910 (19)	−516 (26)	502 (27)	−282 (28)
O	26147 (4)	14655 (6)	38122 (13)	2205 (13)	2926 (17)	3823 (20)	−680 (24)	−1038 (25)	−401 (28)

	x	y	z	U(Å²)		x	y	z	U(Å²)
H(1)	−841 (10)	1571 (12)	−2515 (24)	43 (2)	H(2)	1301 (8)	3624 (11)	14 (21)	34 (2)

Table 3. *Anisotropic type* II *extinction parameters with their e.s.d.'s in parentheses and the lengths of the principal axes of the ellipsoid*

	Tensor component (×10^{-4})	Length of principal axis (×10^{-6} cm)
G_{11}	74 (100)	8·24
G_{22}	94 (61)	7·33
G_{33}	44 (30)	10·8
G_{12}	−79 (71)	
G_{13}	43 (52)	
G_{23}	−36 (34)	

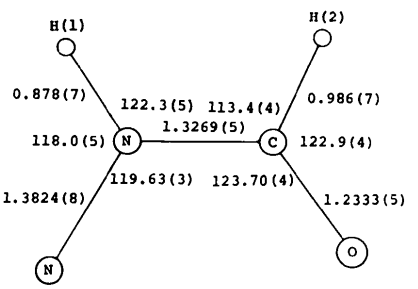

Fig. 2. Bond lengths (Å) and angles (°).

1974). The bond angles around the C atom show significant deviations from 120°, in contrast to those around the N atom.

Errors in the electron-density map

Errors in the electron-density map have the following origins: errors in observed structure amplitudes, error in the scale factor, and the effect of unobserved reflexions.

Possible systematic errors in the structure amplitudes are mainly due to errors in the attenuation factors and errors in the scattering process (such as absorption, extinction and simultaneous-reflexion effects). However, these systematic errors were in practice small, or were made as small as possible as described above. In fact, the intensity deviations among symmetry-related reflexions were suppressed within their statistical counting errors for almost all the reflexions observed in full reciprocal space. The remaining error in the observed structure amplitudes seems to be due to the inhomogeneity of the X-ray beam and to fluctuations of current and voltage in the X-ray tube. Thus the error in observed structure amplitude $\sigma(F_o)$ was estimated as follows:

$$\sigma^2(F_o) = \sigma^2(F_s) + \sigma^2(F_l),$$

where $\sigma(F_s)$ is the error in a short period of time and $\sigma(F_l)$ is that in a long period of time. $\sigma(F_s)$ is defined as the largest value among the statistical counting errors and the intensity differences between symmetry-related reflexions observed in the series. $\sigma(F_l)$ is evaluated from three reference reflexions observed repeatedly throughout the measurement as follows:

$$\sigma(F_l) = |R_i - 1| \times F_o \equiv \Delta R_i \times F_o,$$

where R_i is the largest value of the four ratios of three reference structure amplitudes and their sum, to their mean values. These mean values were weighted mean values, employing as weighting the sum of all the structure amplitudes that were measured after one set and before the next set of the reference reflexions were observed. The largest value of ΔR_i was 0·054. On substituting $\sigma(F_o)$ in the following equation, the error in the electron-density map $\sigma[\rho_o(\mathbf{r})]$ was calculated (Coppens & Hamilton, 1968):

$$\sigma^2[\rho_o(\mathbf{r})] = \sum_{h=-\infty}^{h=\infty} (1 + \cos 4\pi\mathbf{h}.\mathbf{r})\sigma^2(F)/V^2.$$

The calculated error $\sigma(\rho_o)$ was 0·015 e Å^{-3} at the origin and 0·008 to 0·009 e Å^{-3} elsewhere. The larger errors at special positions such as the origin were pointed out by Cruickshank & Rollett (1953) and discussed by Coppens & Hamilton (1968).

Error in the scale factor estimated from the variances of the least-squares fit was negligibly small, though the difference between the scale factor refined by neutron parameters (Tanaka, Marumo, Sato & Saito, 1978) and the conventional X-ray scale factor is about 2·7%.

It is necessary to estimate an error due to unobservable reflexions including series-termination error, because only reflexions with 2θ less than 136° could be observed in the present case owing to mechanical limitations, and limited machine time did not allow us to measure very weak mechanically observable reflexions with sufficient statistical accuracy. This is defined as an expected mean-square error as the first step and is given as

$$\sigma^2(\rho_{\text{unobs}}) = \int (\rho_t - \rho_o)^2 \mathrm{d}V/V,$$

where ρ_t and ρ_o are electron densities calculated with an infinite number of 'true' structure factors and with a finite number of observed structure factors respectively. If the observed structure factor is assumed to contain no error, $\sigma^2(\rho_{\text{unobs}})$ becomes

$$\sigma^2(\rho_{\text{unobs}}) = \sum_{\text{unobs}} |F_{\mathbf{h}}^t|^2/V^2.$$

where the summation means the sum of all the unobservable $F_{\mathbf{h}}^t$'s. When $F_{\mathbf{h}}^t$ was substituted by the calculated structure factor $F_{\mathbf{h}}^c$ and $\sigma[\rho_{\text{unobs}}(s)] = (\sum_{\sin\theta/\lambda=0}^{s} F_{\mathbf{h}}^{c2})^{1/2}/V$ was plotted against $s(\sin\theta/\lambda)$, it was found that $\sigma[\rho_{\text{unobs}}(s)]$ approached asymptotically to 0·10 e Å^{-3} at $\sin\theta/\lambda = 1{\cdot}6$ Å^{-1}. Then, as the second step, the electron-density map was calculated using only the unobservable calculated structure factors with $\sin\theta/\lambda$ less than 1·8 Å^{-1} (depicted in Fig. 3). This map agrees qualitatively with the result expected from the formula of Lipson & Cochran (1953) and indicates that large peaks with heights of 1 to 3 e Å^{-3} occur around atoms, and at the bonding area the electron density of this map ranges from 0·1 to 0·2 e Å^{-3}.

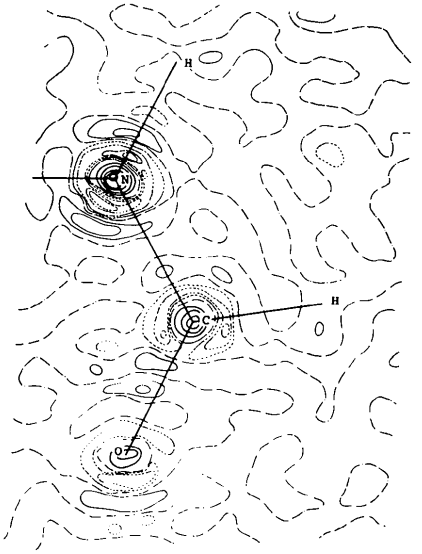

Fig. 3. The electron-density map on the molecular plane calculated using expected structure factors of unobservable reflexions with $\sin\theta/\lambda$ up to 1·8 Å^{-1}. Contours drawn by broken, thin, and thick lines are at intervals of −0·1, 0·1 and 0·5 e Å^{-3} respectively. Dashed–dotted lines are zero contours.

Consequently, it was revealed that in the electron-density map the error due to unobservable reflexions was dominant over other errors; Fig. 3 shows the error of the electron-density map. In the difference-density map, it is expected that the error due to unobservable reflexions is much smaller than those in the electron-density map, because the atomic parameters were determined accurately from a predominantly larger number of reflexions. Thus the error in the difference-density map is concluded to be smaller than that in Fig. 3, and at least larger than the error originating from those in the observed structure amplitudes. Accordingly, all the peaks due to overlap density and lone pairs in Fig. 5 can be taken as significant when compared with those in Fig. 3.

Results and discussion

Residual electron density

In Fig. 4, the difference-density map on the molecular plane without correction for extinction or simultaneous-reflexion effects is depicted, and shows somewhat different features from the final difference-density map shown in Fig. 5 after correction for these effects: there are two unresolved peaks on the N—N bond, a relatively elongated peak on the N—C bond toward the C atom, and the two non-split peaks due to two O lone pairs in Fig. 4. These differences between the two figures indicate the importance of these corrections.

The qualitative features of the final difference-density map in Fig. 5 correspond to the elementary chemical concepts, such as overlap density and lone-pair density. Overlap density is observed in the N—N, N—C and C=O bonds with heights of 0·15, 0·38 and 0·33 e Å^{-3} respectively. They are all significant, as described above.

There are expected to be two lone pairs in the molecular plane around the terminal carbonyl O atom; this is in good agreement with the observed density in Fig. 5. The peak heights are 0·14 and 0·17 e Å^{-3}, which are also significant. The directions of these peaks to the C=O bond are about 90 and 120°. The former is directed toward H(1′) attached to N′ in another half molecule related by the centre of symmetry. The distance between O and H(1′) is 2·393 (4) Å, using the position of H(1′) determined by neutron diffraction (Tanaka *et al.*, 1978).

It is also expected from the hybridization scheme of the N atom that there is a lone pair in the plane perpendicular to the molecular plane. However, no peak due to the lone pair of electrons was observed in the difference-density map. This supports the previous suggestion (Tomiie *et al.*, 1958; Ottersen & Jensen, 1975) that the lone-pair orbitals participate strongly in resonance stabilization of the formamide unit.

From the planarity of the diformohydrazide molecule, it is expected that the N–N, N–C and C=O bonds have π-bond character. Thus it is of interest to examine the difference density at the sections perpendicular to those bonds through the overlap peaks; these are given in Fig. 6 with the sections in the molecular plane. It is striking that all these peaks are elongated in the direction perpendicular to the molecular plane. It might be argued that the elongation represents the extra thermal motion in this section; however, rigid-body analysis of this molecule (Cruickshank, 1956) using the thermal parameters determined by neutron diffraction (Tanaka *et al.*, 1978) reveals the amplitude of the translational vibration perpendicular to the molecular plane to be only 0·20 Å. The extension of the bond peak is therefore attributed to the partial π-bond character of the N–N and N–C bonds. The polarity of the carbonyl bond with O negative and C positive is apparently observed in the difference outer-shell density map shown in Fig. 7. This difference outer-shell density $\Delta\rho_{x-c}$ is defined as

$$\Delta\rho_{x-c}(\mathbf{r}) = \sum (F_{\text{obs}} - F_{\text{core}}) \cos[2\pi\mathbf{H}.\mathbf{r} - \alpha(\mathbf{H})]/V,$$

where $\mathbf{H} = (hkl)$, F_{obs} is the observed X-ray structure amplitude with appropriate phase and F_{core} is the structure factor calculated with isolated-atom X-ray form factors f_c including only the contribution from

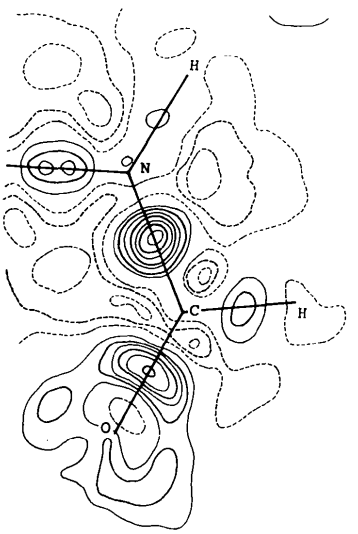

Fig. 4. Difference-density map on the molecular plane without simultaneous-reflexion or extinction corrections. Contours are at intervals of 0·05 e Å^{-3}. Broken lines indicate negative contours.

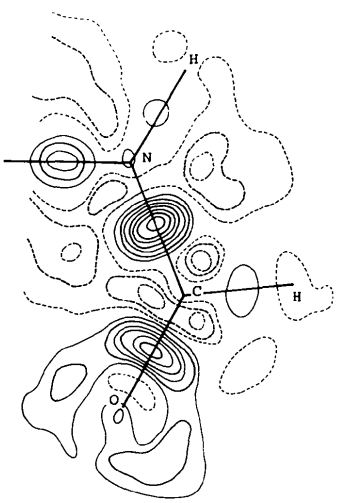

Fig. 5. Final difference-density map on the molecular plane. Contours are at 0·05 e Å^{-3}. Broken lines indicate negative contours.

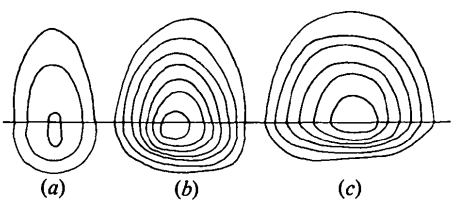

Fig. 6. Difference maps through the tops of the peaks due to overlap density of (*a*) N–N, (*b*) N–C and (*c*) C=O bonds. The lower and upher halves of the diagram indicate sections in and perpendicular to the molecular plane respectively.

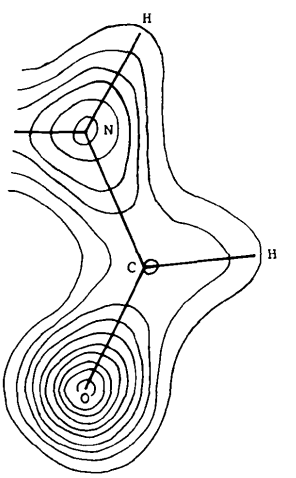

Fig. 7. Difference outer-shell density map on the molecular plane. Contours are at 0·5 e Å^{-3}.

inner-shell electrons, *i.e.* $1s^2$ in the present case. This map shows the sp^2-like distribution of bonding electrons around the N atom along the N–N, N–C and N–H bonds, a deficiency of bonding electrons around the C atom and an excess of electrons around the O atom.

Hydrogen bond

Diformohydrazide molecules are held together by N–H···O hydrogen bonds; H(1)···O is 1·777 (3) Å, N···O is 2·7839 (5) Å and ∠N–H···O is 161·8 (3)° [the position of the H atom is that determined by neutron diffraction (Tanaka *et al.*, 1978)]. The equation of the plane determined by N, H and O is $6{\cdot}298x + 1{\cdot}151y - 3{\cdot}254z = 0{\cdot}5750$, where x, y and z are fractions of the lattice constants. The angle between this plane and the molecular plane is 30·08°. The electron-density map on the plane described above is presented in Fig. 8(*a*). N, H and O atoms are connected by a significant electron cloud, and there is no other inter- or intramolecular non-bonded connexion. This implies a kind of flow of electrons along the N–H···O hydrogen bond. From the difference-density map of the same plane in Fig. 8(*b*) it becomes evident that a large positive peak of 0·15 e Å^{-3} which is due to the O lone pair lies on the line O···H(1), a positive peak of 0·08 e Å^{-3} due to overlap density lies in the middle of the N–H(1) bond and a negative peak of 0·10 e Å^{-3} near the H atom lies towards the O atom.

It is interesting to examine the residual-electron-density map on the plane which is perpendicular to the plane determined by the N, H(1) and O atoms and includes the O···H(1) hydrogen bond. This is depicted in Fig. 9. The straight line in the figure shows the intersection between this plane and the molecular plane.

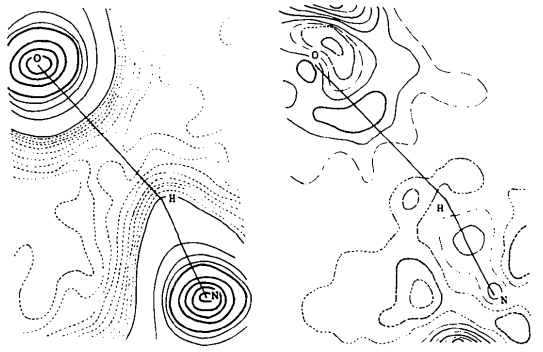

(*a*) (*b*)

Fig. 8. (*a*) Electron-density map on the plane defined by N, H and O atoms forming the N–H···O hydrogen bond. Contours drawn by broken, thin, and thick lines are at intervals of 0·1, 1 and 5 e Å^{-3} respectively. (*b*) Difference-density map on the same plane as (*a*). Contours are at 0·05 e Å^{-3}; broken lines indicate negative contours, and dashed–dotted lines zero contours.

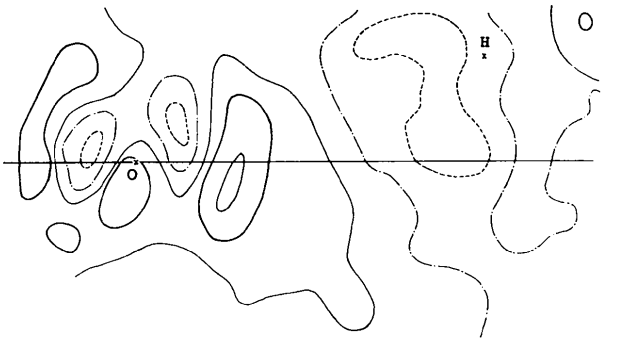

Fig. 9. Difference density map on the plane perpendicular to the hydrogen-bonding plane. Contours are at 0·1 e Å^{-3}. Broken lines indicate negative contours and dashed–dotted lines zero contours.

This might imply that the electron cloud of the O lone-pair electrons does not elongate towards the H atom but lies in the molecular plane. However, further study is necessary on this point.

Effective numbers of electrons

Effective numbers of electrons around each atom or atomic group were calculated by direct integration of electron density. Electrons localized between bonded atoms were also estimated from the residual electron density. The number of electrons n in the volume V_m was calculated as the sum of the electron density $\rho(\mathbf{r}_i)$ weighted by the volume element Δv. The volume element Δv has the shape of a parallelepiped with edges 0·01**a**, 0·01**b** and 0·02**c** for the integration of electron density and 0·005**a**, 0·005**b** and 0·01**c** for that of residual electron density. The boundary planes between bonded atoms were defined as being perpendicular to each bond and passing through the maximum of the peak due to overlap density on the final difference map. The planes that define the exterior boundary of NHCHO were taken in such a way that the points around the molecule with significant electron density were all included. As was described earlier, two diformohydrazide molecules are connected intermolecularly by a significant number of electrons through the N–H···O hydrogen bond; thus the boundary plane between the NH and the O was set so as to be perpendicular to the line linking H(1) with O and to pass through the point with zero electron density on the final difference-density map in Fig. 8(*b*). This plane lies at a distance of 1·00 Å from the O atom. The two boundary planes parallel to the molecular plane were chosen to lie at distances of 1·6 Å above and below it, because it is apparent from the electron-density diagrams on the planes perpendicular to the molecular plane that effective 'molecular electrons' lie within these

Table 4. *Numbers of electrons and residual electrons, and coordinates of the centres of the electron clouds*

(*a*) Numbers of electrons n around atomic groups or atoms, and the numbers of residual electrons Δn (e)

	n Present study	n Tomiie *et al.* (1958)	n Ottersen (1974) (ELS)	n Calculated (CNDO)	Δn Present study	$\Delta n/Z$*
NH	7·845 (4)	7·72	7·69 (21)	7·95	0·152 (4)	
CH	6·755 (7)	6·60	7·04 (25)	6·65	0·167 (7)	
N	6·504 (12)			7·12	0·106 (12)	0·015
C	5·446 (11)			5·60	0·087 (11)	0·015
O	8·409 (42)	8·61	8·27 (21)	8·38	0·361 (42)	0·045
H(1)	1·341 (12)			0·84	0·046 (12)	0·046
H(2)	1·309 (13)			1·05	0·079 (13)	0·079

(*b*) Number of residual electrons Δn due to the overlap density of bonds

	N–N	N–C	C=O
Δn	0·033e	0·080e	0·112e

(*c*) Fractional coordinates of the centres of the electron clouds ($\times 10^5$)

	NH	CH	N	C	O	H(1)	H(2)
x_c	−1332	13462	403	13657	26290	−9745	12648
y_c	11386	24098	10109	21062	14164	17580	36725
z_c	−9870	8845	−5776	11090	38411	−29722	−95

* Z is the atomic number.

areas. Thus V_m's are surrounded by five to seven planes, two of which are placed above and below the molecular plane and are parallel to it, and the rest perpendicular to it, except for the plane between the NH group and the O atom. Outside these boundaries, the electron-density map was flat within $\pm 0{\cdot}1$ e Å^{-3} and a few small peaks had a maximum electron density of 0·2 e Å^{-3}. These ripples amount to only 0·05% of the maximum peak height in $\rho(\mathbf{r})$. The results, together with those obtained by Tomiie *et al.* (1958) and Ottersen (1974), are in Table 4(*a*); the numbers in parentheses are estimated standard deviations which were evaluated from $[\Delta v^2 N\sigma^2(\rho_o) + \Delta\rho_u^2]^{1/2}$, where N is the number of volume elements in V_m, $\Delta\rho_o$ is 0·009 e Å^{-3} as shown before and $\Delta\rho_u$ is the value corrected for the effect of unobservable reflexions described below; results calculated by the CNDO/2 molecular-orbital method using the Fortran program *PHOTOCHEM* (kindly provided by Dr K. Seki) are also listed. The sum of the observed numbers of electrons around NH, CH and O is 23·01 (5), which is in precise agreement with 23, the total number of electrons in the NHCHO moiety. This indicates that the observed electron density has few ghost peaks and, furthermore, that the exterior boundary planes of the NHCHO moiety are defined quite reasonably.

In order to see the effect of unobservable reflexions on the number of electrons, the number of electrons was also calculated on the basis of the calculated structure factors of unobservable reflexions. The results are: NH −0·004, CH −0·007, N 0·012, C 0·011, and O −0·042 e. In contrast to the large ripples around atoms in Fig. 3, the unobservable reflexions have little effect on the integrated number of electrons because of the balance of plus and minus peaks, which agrees qualitatively with the previous formulation of termination error by Sakurai (1965).

The numbers of residual electrons Δn in the same integrated volume were calculated as the sum of the positive electron density $\rho(\mathbf{r}_i)$ only, weighted by the volume element Δv and are listed in Table 4(*a*). The ratios of the numbers of residual electrons around atoms to their atomic numbers are also included in the table. These values may indicate a measure of the extent of the asphericity of electron distribution of these atoms due to bond formation, lone pairs and delocalization of electrons. In Table 4(*b*), the numbers of residual electrons due to overlap density are tabulated. In this case, the integrated volume was defined as being surrounded by six planes so that the residual peak due to overlap density was included.

The centres (x_c,y_c,z_c) of the electron cloud around atoms or atomic groups were calculated by the relation $\mathbf{r}_c = \sum_i \mathbf{r}_i\rho(\mathbf{r}_i)\Delta v/\sum_i \rho(\mathbf{r}_i)\Delta v$, where $\mathbf{r}_c = (x_c,y_c,z_c)$, and are listed in Table 4(*c*). Those of the N, C and O atoms are nearly the same as the atomic positions determined by X-ray and neutron diffraction methods. However, those of the two H atoms are closer to the atomic

positions obtained by the neutron method than those by the X-ray method. The calculated distances between the centres of electron clouds are N–H = 1·08 and C–H = 1·05 Å, while the N–H and C–H bond lengths determined by neutron diffraction (Tanaka *et al.*, 1978) are 1·038 (3) and 1·095 (5) Å respectively.

It is shown in Table 4(*a*) that the O atom is negative to the extent of 0·41 e and N and C atoms are positive to the extent of 0·50 and 0·55 e respectively. Two H atoms are negative and the NH and the CH groups are positive, and the polarity of the carbonyl group is apparent. The most significant difference between the results of the direct-integration method and the calculation by the CNDO/2 method is that the charge of the N atom is positive in the former and negative in the latter. This may result from the difference of the two methods. The direct-integration method assumes that electrons in the neighbourhood of the atom belong to it and the delocalized electrons are not taken into account.

The numbers of electrons and the centres of the electron clouds are strongly dependent on the choice of the boundary planes. However, the boundary plane between N and H(1) was placed at a distance of 0·59 Å from N and 0·45 Å from H(1). The radial charge densities of the 1*s* orbital of the H atom and that of the 2*s* orbital of the N atom have their maximum values at 0·53 and 0·56 Å, respectively, from the atomic nuclei (Slater, 1960). Thus, the deficiency of electrons around the N atom seems to be due not to the failure of the boundary-plane setting but to the effusion of electrons of the N atom to the O atom through the N–C=O conjugation system and N–H···O hydrogen bonding. The centre of the electron cloud of H(1) is attracted towards the O atom. This, together with the electron-density map in Fig. 8(*a*), implies a flow of electrons between the NH group and the O atom.

The numbers of residual electrons, which show the asphericity of the electron-density distribution around each atom, become more prominent in the sequence C, N and O, which is in agreement with the extent of asphericities of the electron-density distribution expected from the electron configuration of these atoms. The numbers of residual electrons due to overlap density of bonds are in the sequence of the overlap densities of the C=O, N–C and N–N bonds.

The author wishes to express his sincerest gratitude to Professor Y. Saito for his continuous encouragement and valuable advice and also to Professor F. Marumo for his encouragement.

References

AINSWORTH, C. & JONES, R. G. (1955). *J. Am. Chem. Soc.* **77**, 621–624.

CLEMENTI, E. (1965). *Tables of Atomic Functions*; *IBM J. Res. Dev.* **9** (supplement).

COPPENS, P. & HAMILTON, W. C. (1968). *Acta Cryst.* B**24**, 925–929.

COPPENS, P. & HAMILTON, W. C. (1970). *Acta Cryst.* A**26**, 71–83.

CRUICKSHANK, D. W. J. (1956). *Acta Cryst.* **9**, 754–756.

CRUICKSHANK, D. W. J. & ROLLETT, J. S. (1953). *Acta Cryst.* **6**, 705–707.

FUKAMACHI, T. (1969). *Jpn. J. Appl. Phys.* **8**, 851–854.

FUKAMACHI, T. (1971). Tech. Rep. B, No. 12. Institute for Solid-State Physics.

LIPSON, H. & COCHRAN, W. (1953). *The Determination of Crystal Structures*, p. 324. London: Bell.

OTTERSEN, T. (1974). *Acta Chem. Scand. Ser. A*, **28**, 1145–1149.

OTTERSEN, T. & JENSEN, H. H. (1975). *J. Mol. Struct.* **26**, 355–363.

SAKURAI, T. (1965). *Acta Cryst.* **19**, 320–330.

SHOEMAKER, D. (1968). *Acta Cryst.* A**24**, 136–142.

SLATER, J. C. (1960). *Quantum Theory of Atomic Structure*, Vol. I. New York: McGraw–Hill.

STEWART, R. F., DAVIDSON, E. R. & SIMPSON, W. T. (1965). *J. Chem. Phys.* **42**, 3175–3187.

TANAKA, K., MARUMO, F., SATO, S. & SAITO, Y. (1978). To be published.

TANAKA, K. & SAITO, Y. (1975). *Acta Cryst.* A**31**, 841–845.

TOMIIE, Y. (1958). *Acta Cryst.* **11**, 875–882.

TOMIIE, Y., KOO, C. H. & NITTA, I. (1958). *Acta Cryst.* **11**, 774–781.

ZACHARIASEN, W. H. (1967). *Acta Cryst.* **23**, 558–564.